Supporting Information

Chen et al. 10.1073/pnas.1001721107

SI Text

SI Material and Methods. ***Plasmid construction.*** All plasmids were constructed by using standard molecular biology techniques (1). Plasmid maps are provided in Fig. S8. All oligonucleotides were synthesized by Integrated DNA Technologies, and all constructs were sequence verified (Laragen, Inc.). Cloning enzymes, including restriction enzymes and T4 DNA ligase, were obtained from New England Biolabs, and DNA polymerases were obtained from Stratagene.

A fusion of the firefly luciferase (*ffluc*) gene and the *Sh ble* gene encoding zeocin resistance was PCR amplified from pMOD-LucSh (Invivogen) by using forward and reverse primers Kozak BamHI5′ (5′ATCGGATCCGCCGCCACCATGGA GGATGCCAAGAATATTAAGAAAGG) and zeocin XbaI3′ (5′ TATTCTAGATCAGT CCTGCTCCTCTGCCACAAAGTGC), respectively. The plasmid pffLuc:zeo was constructed by inserting the resulting PCR product into pcDNA3.1(+) (Invitrogen) via the unique restriction sites BamHI and XbaI located in the multicloning site behind the CMV promoter.

The *cd19* gene was PCR amplified from CD19t-Tk-T2A-IL15op_epHIV7 by using forward and reverse primers CD19t BlpI5′ (5′ ATTGCTGAGCCTAGAGCTGAAG) and CD19t-mutsr39TK FR (5′CCCGCAGTAGCGTGGGCATTCTTTTCCTCCTCAGGAC CAG), respectively. The thymidine kinase gene *mutsr39tk* was PCR amplified from mutsr39tk_pcDNA3.1(+) by using forward and reverse primers CD19t-mutsr39TK FF (5′C TGGTCCTGAGGAGGAAAAGAATGCCCACGCTACTGCGGG) and mutsr39TK-T2A FR (5′CCTCTCCGCCGCCAGATCTGTTAGCCTCCCCCATCTCCC), respectively. The cytokine gene *il-15* was PCR amplified from CD19t-Tk-T2A-IL15op_epHIV7 by using forward and reverse primers mutsr39TK FF (5′GGGAGATGGG GGAGGCTAACAGATCTGGCGGCGGAGAGG) and IL15op BsrGI3′ (5′TCTCGGTG TACAGGGTGGCG), respectively. PCR products for the three genes were assembled via a fourth PCR reaction by using forward and reverse primers CD19t BlpI5′ and IL15op BsrGI3′, respectively. The plasmid pIL15 was constructed by inserting the assembled PCR product (*cd19-mutsr39tk-t2a-il15*) into CD19t-Tk-T2A-IL15op_epHIV7 via the unique restriction sites BlpI and BsrGI behind the EF1α promoter.

The fluorescence gene *egfp* was PCR amplified from eGFP_pcDNA3.1(+) by using forward and reverse primers eGFP KpnI5′ (5′CTTGGTACCCGCCACCATGGTGAGC AAG) and T2A-IL2 FR (5′CCACGTCACCGCATGTTAGAAGACTTCCTCTGCCCTC TCCGCTGCCCTTGTACAGCTCGTCCATGCC), respectively. The cytokine gene *il-2* was PCR amplified from IL2_pSK by using forward and reverse primers T2A-IL2 FF (5′ CT TCTAACATGCGGTGACGTGGAGGAGAATCCCGGCCCTATGTACAGGATGCAACTCCTGTC) and IL2 XhoI3′ (5′ AGACTCGAGTCAAGTTAGTGTTGAGATGATGC), respectively. PCR products for the two genes were assembled via a third PCR reaction by using forward and reverse primers eGFP KpnI5′ and IL2 XhoI3′, respectively. The plasmid eGFP-T2A-IL2_pcDNA3.1(+) was constructed by inserting the assembled PCR product (*egfp-t2a-il2*) into pcDNA3.1(+) via the unique restriction sites KpnI and XhoI behind the CMV promoter. A DNA sequence including the CMV promoter, the *egfp-t2a-il2* fusion gene, and the poly-A sequence was PCR amplified from eGFP-T2A-IL2_pcDNA3.1(+) by using forward and reverse primers CMV HpaI5′ (5′AATAGTTAAC GTTGACATTGATTATTGACTAGTTATTAATAGTAATCAA) and bGHpA SacII3′ (5′AATACCGCGGCCATAGAGCCCACCGC), respectively. The PCR product was inserted into dsRed Express_pcDNA3.1(+) via the unique restriction sites HpaI and SacII. The CMV promoter regulating the *egfp-t2a-il2* fusion gene was replaced by the EF1α promoter via the unique restriction sites BglII and KpnI to construct the plasmid pIL2. The EF1α promoter sequence was PCR amplified from pIL15 by using forward and reverse primers EF1α BglII5′ (5′AATAGATATCTGCTTCGCGAGGATCTGC) and EF1 α KpnI3′ (5′AATAGGTACCGGTGGCGGCGCTAG), respectively.

A standardized cloning method was developed to allow for the sequential insertion of engineered ribozyme switches and corresponding control constructs in the 3′ UTR of the target transgenes. The engineered ribozyme switch constructs were generated by PCR amplification by using the forward primer Rz XhoI-AsiSI5′ (5′AATACTCGAG GCGATCGC*AAACAAACAAA*), where the underlined sequences indicate restriction sites for XhoI and AsiSI, respectively, and the reverse primer Rz ApaI-PacI3′ (5′AATA GGGCCCAAGATTAATTAA*AAAAAAAATTTTTATTTTTCTTTTT*GCTGTT), where the underlined sequences indicate restriction sites for ApaI and PacI, respectively. The italicized sequences indicate spacers flanking each ribozyme switch, and the 3′ spacer sequence forms a hairpin structure consisting of A-U pairs to provide insulation for each ribozyme switch. The first copy of an engineered ribozyme switch in each plasmid (using pIL2 or pIL15 as the plasmid backbone) was inserted via the unique restriction sites XbaI and ApaI. All subsequent copies of the engineered ribozyme switches were inserted behind the 3′ end of the previous copy of ribozyme switch by digesting the plasmid with PacI and ApaI and the insert with AsiSI and ApaI, where digestion with PacI and AsiSI results in identical sticky ends. The resulting ligation product retained unique PacI and ApaI sites while eliminating the AsiSI site, thus allowing the cloning strategy to be repeated for each additional copy of the ribozyme switch inserted into the construct.

Transient transfection and fluorescence quantification. All transient transfections into CTLL-2 cells were performed with an Amaxa Nucleofector II and the Mouse T Cell Nucleofector Kit (Amaxa) following the manufacturer's protocols. Electroporations were performed with 2×10^6 cells and 3 μg of plasmid DNA. One hour after electroporation, samples were diluted 2-fold with supplemented RPMI medium 1640 and split into two wells, one treated with small-molecule input and one without input. In experiments testing a range of input concentrations, multiple aliquots of cells were electroporated as described. One hour after electroporation, samples were combined, diluted 2-fold, split into the appropriate number of wells, and each treated with the appropriate concentration of small-molecule input. Fluorescence and cell viability data were obtained 24 and 48 hours after transfection, respectively, by using a Quanta Cell Lab Flow Cytometer (Beckman Coulter) equipped with a 488-nm laser. EGFP, phycoerythrin (PE), and dsRed-Express were measured through 525/30-nm band-pass, 575/30-nm band-pass, and 610-nm long-pass filters, respectively. Viability was gated on the basis of side scatter and electronic volume, and only viable cells were included in fluorescence measurements. For samples expressing constructs derived from pIL2, viable cells were further gated for dsRed-Express expression, which served as a transfection efficiency control, before EGFP intensity values were collected. All fluorescence measurements were reported as the geometric mean intensity observed in the gated population. To control for toxicity and other possible nonspecific effects of transfection and input ligand

molecules, cells transfected with an inactive (scrambled) hammerhead ribozyme and treated with the corresponding concentration of ligand molecule served as positive controls to which values from cells transfected with active ribozyme switches were normalized. The inactive ribozyme constructs provide controls for the maximum possible gene expression levels from the ribozyme-based regulatory systems. CD19 antibody staining was performed by washing 1×10^6 cells twice with 500 μL HBSS (Gibco), incubating with 10 μL PE-conjugated CD19 antibody (Beckman Coulter) in 50 μL HBSS for 15 minutes at 4 °C in the dark, washing twice with 500 μL HBSS, and analyzing on the flow cytometer. Transient transfection experiments were performed with at least two replicate samples, and reported error bars indicate 1 standard deviation from the averaged measured value normalized by the inactive ribozyme control.

Stable CTLL-2 cell line generation. To generate a CTLL-2 cell line for in vivo imaging, CTLL-2 cells were electroporated with the pffLuc:zeo plasmid, and stable integrants were selected on the basis of resistance to 0.1 mg/mL zeocin. The stable cell line CffLuc was confirmed through a luciferase activity assay, in which 1×10^4 cells were resuspended in 100 μL media and aliquoted into 96-well black, clear-bottom plates. Each well was incubated with 20 μL of 1.4 mg/mL D-luciferin diluted in PBS (Xenogen) at 37 °C for 10 minutes, and luciferase signal was detected by using a Victor3 1420 Multilabel Counter (Perkin Elmer). Signals from six replicates were averaged for each experiment, and CTLL-2 cells not expressing *ffluc* were used as negative controls.

To generate CTLL-2 cells stably expressing constructs encoding the T-cell proliferation regulatory system for in vivo imaging, CffLuc cells were electroporated with plasmids derived from the pIL15 plasmid and linearized at the unique NsiI site. Electroporations for stable cell lines were carried out in seven cuvettes, each containing 5×10^6 cells and 5 μg plasmid DNA. One hour after electroporation, all electroporated samples were combined, diluted to a total volume of 50 mL, and supplemented with IL-2 every 48 hours to a final concentration of 100 U/mL. Cells were stained with PE-conjugated CD19 antibodies 7 days after electroporation and sorted for PE+ cells by FACS by using a BD FACSAria cell sorter (BD Biosciences) equipped with a 488-nm laser. The sorted cells were grown for 13 days and then stained and further sorted via magnetism-automated cell sorting (MACS) by using an autoMACS Separator (Miltenyi Biotec) for PE+ cells. Theophylline was added to cell cultures to a final concentration of 250 μM 2 days prior to each sort.

Following the FACS and MACS sorts, a series of selection cycles were performed by alternating between growth in ganciclovir and theophylline. Cells were grown for 2 weeks following autoMACS sorting in media supplemented with IL-2 every 48 hours to a final concentration of 100 U/mL. The cells were then grown for 7 days in the presence of 1 μM ganciclovir and supplemented with IL-2 every 48 hours to a final concentration of 100 U/mL. The cells were subsequently placed in fresh media supplemented with 250 μM theophylline and allowed to grow for 4 days in the absence of IL-2. Following termination of theophylline treatment, the cells were placed in fresh media supplemented with 100 U/mL IL-2 (added every 48 hours) and 5 μM ganciclovir for 4 days. The theophylline treatment regime then resumed for 8 days, followed by the ganciclovir treatment regime (at 5 μM) for 10 days and a final theophylline regime for 5 days. Cell density was maintained between 0.05×10^6 and 0.5×10^6 cells/mL throughout the cell culture procedure. Following the last theophylline treatment regime, cells were stained with PE-conjugated CD19 antibodies and sorted for single clones into 96-well plates by FACS for low, medium, and high PE levels. The sorted clones (CffLuc-pIL15) were grown in media supplemented with 250 μM theophylline, 50 U/mL penicillin:streptomycin, and no IL-2. Clones were expanded from the low PE fractions into larger culture volumes and finally maintained in T75 tissue culture flasks (BD Falcon).

In vitro growth assay for stable CTLL-2 cell lines. CffLuc-pIL15 clones were cultured under regular conditions (RPMI 1640 media supplemented with 100 U/mL IL-2 every 48 hours, 0.2 mg/mL zeocin, no theophylline), washed twice with HBSS, and split into five identical aliquots in 6-well plates at approximately 0.01×10^6 cells/mL (4 mL/well). Each well was supplemented with one of the following: 100 U/mL IL-2, 100 μM theophylline, 250 μM theophylline, 400 μM theophylline, or no IL-2 and no theophylline. Cells were split and passaged as necessary into new 6-well plates at approximately 0.03×10^6 cells/mL, and IL-2 was added to the appropriate wells to a final concentration of 100 U/mL every 48 hours. Cell count was obtained from 50 μL of each culture daily for 7 days on a Quanta Cell Lab Flow Cytometer by gating for viable cells on the basis of side scatter and electronic volume. Cell density was calculated by dividing the number of detected live cells by the volume analyzed on the flow cytometer.

CTLL-2 time-course study. CTLL-2 parental cells, clonal stable cell line 1264-48 [L2bulge9(3×)], and clonal stable cell line 1266-3 (inactive ribozyme) were cultured under regular conditions. On day 0, cells were counted for density and washed twice with HBSS. Each cell line was used to seed two 50-mL cultures at 0.15×10^6 cells/mL (set 1) and two 50-mL cultures at 0.05×10^6 cells/mL (set 2). One flask at each seeding density was treated with 500 μM theophylline. Set 1 flasks and set 2 flasks were supplemented with 50 and 100 U/mL IL-2, respectively, to keep IL-2 concentration consistent with seeding cell density and harvesting schedule. On day 1, set 1 flasks were harvested for CD19 antibody staining (1×10^6 cells per sample) and for cell pellet collection for qRT-PCR (12.5×10^6 cells per sample, washed once with HBSS, and flash frozen with liquid nitrogen). Each culture was split to 0.05×10^6 cells/mL at 50 mL total and supplemented with 100 U/mL IL-2 and the appropriate concentration of theophylline (0 or 500 μM). On day 2, the same harvest and subculture procedures were repeated for set 2 flasks. All cultures were treated in this manner every 48 hours until day 7. On day 7, the cell count was obtained for all cultures. After harvesting from set 1 flasks, all cultures were washed twice with HBSS and resuspended in fresh media without theophylline. Set 1 flasks were seeded at 0.05×10^6 cells/mL and supplemented with 100 U/mL IL-2. Set 2 flasks were seeded with all available cells and supplemented with 50 U/mL IL-2. On days 8 and 9, the same harvest and subculture procedures were performed on set 2 and set 1 flasks, respectively. All cultures were treated in this manner every 48 hours until day 14. On day 14, the cell count was obtained for all cultures. After harvesting from set 2 flasks, all cultures were washed twice with HBSS and resuspended in fresh media. All cultures that had been treated with theophylline on days 0–7 were supplemented with 500 μM theophylline on day 14. Set 2 flasks were seeded at 0.05×10^6 cells/mL and supplemented with 100 U/mL IL-2. Set 1 flasks were seeded with all available cells and supplemented with 50 U/mL IL-2. On days 15 and 16, samples were harvested for CD19 staining and subcultured as before for set 2 and set 1 flasks, respectively. All cultures were treated in this manner every 48 hours until day 18.

Transcript analysis through qRT-PCR. mRNA was purified from frozen cell pellets with the GenElute Direct mRNA MiniPrep Kit (Sigma) following the manufacturer's protocols. mRNA samples were treated with 100 U/mL DNaseI at 37 °C for 15 minutes and purified by phenol-chloroform extraction and ethanol precipitation. Reverse transcription was performed with 300 ng mRNA, 2 pmol of each primer, 10 nmol dNTP, 40 U RNaseOUT,

5 mM DTT, 1× First-Strand Buffer, and 200 U SuperScript III Reverse Transcriptase (Invitrogen) in a 20 μL reaction following the manufacturer's protocols. Gene-specific primers (Hprt1 reverse, 5′TGCTGCCATTGTCGAACA; IL-15 reverse, 5′GGTGTCGTGGATGCTG) were used in the cDNA synthesis reactions. The resulting cDNA samples were subsequently treated with 2.5 U of RNaseH at 37 °C for 20 minutes, followed by heat inactivation at 65 °C for 20 minutes.

qRT-PCR reactions were performed in a 25 μL reaction with 200 nM of each primer, 5 μL cDNA, and 1× SYBR Green SuperMix (Bio-Rad) on an iCycler Real-Time PCR machine (Bio-Rad). Separate reactions were performed for the housekeeping gene *Hprt1* (Hprt1 forward, 5′AGCCAGCGAAGCCAC; Hprt1 reverse) and the target gene *il-15* (IL-15 forward, 5′CAACTGGGTGAACGTGAT; IL-15 reverse). The qRT-PCR protocol included 32 cycles of a 15-second annealing step at 50 °C and a 30-second extension step at 72 °C, followed by a melt curve analysis to verify absence of nonspecific products. All reactions were performed in triplicate, and threshold cycle (C_t) values were averaged to obtain the arithmetic mean. Relative IL-15 expression levels were calculated with the following formula (2):

$$\mathrm{RE} = \frac{\varepsilon_{\mathrm{Hprt1}}^{(C_{t,\mathrm{Hprt1}})}}{\varepsilon_{\mathrm{IL\text{-}15}}^{(C_{t,\mathrm{IL\text{-}15}})}},$$

where RE indicates relative IL-15 expression, ε_x indicates primer efficiency for gene x, and $C_{t,x}$ indicates the averaged C_t value for gene x. Standard deviation was calculated with the following formula:

$$\mathrm{STD} = \sqrt{[\mathrm{RE}\ln(\varepsilon_{\mathrm{Hprt1}})]^2(\mathrm{Std}_{\mathrm{Hprt1}})^2 + [\mathrm{RE}\ln(\varepsilon_{\mathrm{IL\text{-}15}})]^2(\mathrm{Std}_{\mathrm{IL\text{-}15}})^2},$$

where STD indicates standard deviation in relative IL-15 expression and Std_x indicates standard deviation calculated from the triplicate samples for gene x. Reported error bars indicate 1 standard deviation.

Western blot analysis of STAT5 levels. Clonal stable cell lines were cultured under regular conditions (see above), washed twice with HBSS, and split into two identical aliquots. The aliquots were grown in the absence of IL-2 and either in the presence or absence of 500 μM theophylline for 3 days. Approximately 2×10^6 cells of each sample were harvested and washed with 1 mL HBSS each day, frozen with liquid nitrogen, and stored at −80 °C until lysis. Cell pellets were lysed with 50 μL Triton-X lysis buffer (1% Triton-X, 10 mM Tris-HCl, pH 7.4, 130 mM NaCl, 5 mM EDTA, protease inhibitor, 5% phosphatase inhibitor cocktail II) and incubated on ice for 1 hour. Lysates were centrifuged at $14,000 \times g$ for 20 minutes at 4 °C. The supernatant was collected and immediately frozen at −80 °C.

Lysate samples were thawed on ice and a standard Bradford assay using Protein Assay Dye (Bio-Rad) was performed with a BSA standard to determine protein concentrations. Samples were run on NuPAGE 4–12% Bis-Tris Gels (Invitrogen) at 90 V for 2.5 hours, where 50 μg of protein from each sample was loaded. Blotting was performed with Mini Trans-Blot Filter Paper (Bio-Rad) and 0.45 μm Nitrocellulose Membranes (Bio-Rad) wetted with NuPAGE transfer buffer (Invitrogen) and transferred at 40 mA per gel with a Hoefer Semi-Phor Blotter (Hoefer Scientific Instruments). Membranes were blocked with Odyssey Blocking Buffer (Li-Cor) at 4 °C for 1 hour and probed with Rabbit-anti-pSTAT5 antibody (Cell Signaling) or IRDye 800CW-conjugated anti-β-actin antibody (Rockland) at 4 °C overnight in the dark. Membranes probed with p-STAT5 antibodies were washed 4 times with 100 mL TTBS (1× TBS; Bio-RAD), 0.1% Tween 20 (Sigma), and further stained with IRDye 800CW-conjugated goat-anti-rabbit antibody (Li-Cor) at room temperature for 1 hour. Membranes stained for β-actin and p-STAT5 were washed 4 times with 100 mL TTBS and once with 100 mL TBS before fluorescent images were acquired and quantified with the Odyssey Infrared Imaging System (Li-Cor). Integrated band intensity was calculated with the Odyssey system by using blank gel areas surrounding each band for background subtraction. Relative p-STAT5 expression levels were calculated by normalizing the integrated intensity of the p-STAT5 band by that of the β-actin band from the same protein sample. Data shown are representative of two independent experiments.

In vivo T-cell proliferation studies in NOD/SCID-IL2(ko) mice. Various CffLuc-pIL15 cell lines, CffLuc, and a CffLuc-derived cell line stably expressing a cytokine fusion transgene with an inactive ribozyme in the 3′ UTR of the transgene were expanded under regular culture conditions. Cells were harvested by centrifugation at 1,200 rpm at 4 °C for 10 minutes, washed twice with PBS, resuspended in PBS at a concentration of 2×10^6 cells/mL, and split into two 50-μL aliquots. Each aliquot was mixed with 50 μL of either PBS or 2 mM theophylline dissolved in PBS. The 100-μL cell suspension was then mixed with 100 μL of Matrigel (BD Biosciences), for a total of 0.1×10^6 cells at a final concentration of 0 or 500 μM theophylline. The cell suspensions were injected subcutaneously (s.c.) into the right or left flank of NOD/scid-IL2(ko) mice. All mice were 8–10 weeks old and bred in the City of Hope lab animal breeding facility, and experiment protocols were approved by the City of Hope Institute Animal Care and Use Committee. In vivo growth of the injected cells was monitored by biophotonic imaging. Clone 1264-48 and the positive control cell line expressing an inactive ribozyme were tested in a second experiment following the procedure described above. Each cell line was injected into both flanks of three mice either with or without 500 μM theophylline, generating six replicates for each experimental condition. One of the mice injected with clone 1264-48 without theophylline exhibited abnormally large engraftments in both flanks. Additional subjects were studied to verify that cell growth in this mouse was aberrant in a statistically significant manner ($P = 0.044$ on the basis of comparison against eight other replicates with the same experimental condition), and data from this mouse were excluded from statistical analyses of the ribozyme switch system.

Biophotonic in vivo imaging. Animals received intraperitoneal (i.p.) injections of 4.29 mg per mouse of freshly prepared luciferin substrate (Caliper Life Sciences) suspended in 150 μL of PBS. Mice were then anesthetized with isoflurane (1.5 L oxygen+ 4% isoflurane per minute) in an induction chamber. After induction of deep anesthesia, mice were imaged by using the IVIS Imaging System 100 Series (Xenogen) consisting of a CCD camera mounted on a light-tight specimen chamber (darkbox), a camera controller, a camera cooling system, and a Windows computer system for data acquisition and analysis. Images were acquired at 10–20 minutes after luciferin injection with the appropriate exposure time and binning mode to prevent signal saturation. Luciferase activity was analyzed through Living Image Software 3.1 from Xenogen to quantify tumor region flux (photons per second).

Statistical analysis. Statistical analysis was performed on growth rate data by using the Mann–Whitney U test to calculate two-tailed P values. The doubling time of injected cells was calculated on the basis of the total luciferase signal flux data collected over the course of each in vivo study. Signal flux data were fitted to an exponential curve, and the resulting equation was used to calculate cell-doubling time by using the equation:

$$t_D = (t_2 - t_1)\frac{\log(2)}{\log(F_2 - F_1)},$$

where t is time, F is signal flux, and t_D is doubling time.

Lentivirus production. HEK 293T cells were seeded at 5.0×10^6 cells in 9 mL per 10-cm tissue culture plate and transfected with 1 mL solution containing vector DNA, 62 mM $CaCl_2$, and 1× Hepes buffered saline. Cells were washed twice with 5 mL 1× PBS without magnesium and calcium the following morning and fed 10 mL of complete DMEM with 60 mM sodium butyrate. At 24, 48, and 72 hours posttransfection, viral supernatants were harvested by centrifugation at 2,000 rpm for 10 minutes at 4 °C and filtered through a 0.45-μM vacuum filtration unit. Viral supernatants from all time points were pooled and mixed with ¼ volume of 40% PEG. After rotating overnight at 4 °C, samples were centrifuged at 3,000 rpm for 20 minutes at 4 °C and the supernatants discarded. Pellets were resuspended in 35 mL serum-free DMEM and ultracentrifuged at 24,500 rpm for 1.5 hours at 4 °C. Resulting pellets were resuspended in 50 μL serum-free FBS and vortexed at 4 °C for 2 hours. Then 10% FBS was added and the samples stored at −80 °C until titering and use.

Derivation of central memory T (T_{CM}) cells from human peripheral blood mononuclear cells (PBMCs). PBMCs were isolated from donor apheresis products, and 5×10^8 cells were washed twice with 35 mL MACS buffer (2 mM EDTA and 0.5% BSA in PBS) and resuspended in 1.5 mL MACS buffer. Washed cells were stained with 0.75 mL each of CD4, CD14, and CD45RA microbeads (Miltenyi Biotec) and depleted for CD4, CD14, and CD45RA by using an autoMACS Separator (Miltenyi). Depleted cells were washed once with 35 mL MACS buffer, resuspended in 3.5 mL MACS buffer with 10.5 μL anti-CD62L DREG56-biotin antibody (City of Hope Center for Biomedicine and Genetics), and incubated for 20 minutes in the dark at 4 °C. Cells were washed twice with 35 mL MACS buffer and resuspended in 1.2 mL MACS buffer with 300 μL antibiotin microbeads (Miltenyi). Cells were enriched for CD62L by using an autoMACS Separator, placed in fresh RPMI 1640 media supplemented with 10% FBS and stored in a 37 °C incubator.

Lentiviral transduction of T_{CM} cells. T_{CM} cells were seeded at 0.5×10^6 cells in 500 μL per well in a 48-well plate. One and a half million anti-CD3/anti-CD28 Dynabeads (Invitrogen) were washed with 1% heat-inactivated human serum in PBS (pH 7.4), resuspended in 500 μL T-cell media (RPMI 1640 supplemented with 10% heat-inactivated fetal bovine serum) containing 0.5×10^6 T_{CM} cells, and added to each of two wells in a 48-well plate. Each well was fed with 50 U/mL IL-2 and 0.5 ng/mL IL-15, infected with viruses at a multiplicity of infection of 5, and treated with protamine sulfate at a final concentration of 5 μg/mL. The plate was centrifuged at 2,100 rpm for 30 minutes at 32 °C and incubated at 37 °C for 4 hours. Each well was supplemented with 500 μL of warm T-cell media, and the plate was incubated at 37 °C. Cells were assayed by flow cytometry on day 8 posttransduction and Dynabeads were removed on day 14 posttransduction.

T_{CM} cell time-course study. T_{CM} cells transduced with the *cd19-t2a-il15*-L2bulge9(3×) or *cd19-t2a-il15*-inactive ribozyme constructs were stimulated with 100×10^6 PBMCs, 10×10^6 TM-LCLs, and 30 ng/mL OKT2 for each T75 flask and cultured under regular conditions for 12 days. On day 12 poststimulation, each cell line was washed twice with HBSS and used to seed 25-mL cultures at 0.45×10^6 cells/mL. Cell media were supplemented with either no theophylline or 500 μM theophylline, and no IL-2 or IL-15 was added. The CD19 expression level study was performed with duplicate cultures, and the apoptosis staining study was performed with triplicate cultures. Each culture was sampled every 24 hours for antibody staining with PE-conjugated CD19 antibody (Beckman Coulter). For the apoptosis study, CD19-stained samples where subsequently stained with Pacific Blue-conjugated annexin V and SYTOX AAD dead cell stain (Invitrogen) following manufacturer's protocols. Fluorescence data were obtained by using a Quanta Cell Lab Flow Cytometer (Beckman Coulter) with both a 488-nm laser and an UV arc lamp. Pacific Blue, PE, and SYTOX AAD were detected through 465/30-nm band-pass, 575/30-nm band-pass, and 610-nm long-pass filters, respectively. The percent CD19 expression was calculated by measuring the PE expression level of PE+ gated cells and normalizing results of the L2bulge9(3×) sample by those of the inactive ribozyme sample cultured at the same theophylline concentration. Only SYTOX AAD- cells were included in data analyses for the apoptosis study. The population of live CD19+ cells was determined by gating for annexin V−/PE+ cells, and the population of apoptotic CD19+ cells was determined by gating for annexin V+/PE+ cells. Relative population distribution was calculated by normalizing results of the L2bulge9 (3×) sample to those of the inactive ribozyme sample cultured at the same theophylline concentration.

T2A sequences.

T2A DNA sequence.
GGCAGCGGAGAGGGCAGAGGAAGTCTTCTAACATGC-GGTGACGTGGAGGAGAATCCCGG

T2A peptide sequence.
GSGEGRGSLLTCGDVEENPG

Ribozyme switch sequences. Italicized, spacer sequences; underlined, restriction sites.

sTRSV hammerhead ribozyme.
5′CTCGAG *AAACAAACAAA* GCTGTCACCGGATGTGCTT-TCCGGTCTGATGAGT CCGTGAGGACGAAACAGC *AAA-AAGAAAAATAAAAATTTTTTGGAA* TCTAGA

L2bulge1.
5′CTCGAG GCGATCGC *AAACAAACAAA* GCTGTCACCG-GATGTGCTTTCCGGTCTGATGAGTCCGTGTCCATACCA-GCATCGTCTTGATGCCCTTGGCAGGGACGGGACGAG-GACGAAACAGC *AAAAAGAAAAATAAAAATTTTTTTT* TT-AATTAA TCTT GGGCCC

L2bulge8.
5′CTCGAG GCGATCGC *AAACAAACAAA* GCTGTCACCG-GATGTGCTTTCCGGTCTGATGAGTCCGTTGTCCATACC-AGCATCGTCTTGATGCCCTTGGCAGGGACGGGACGG-AGGACGAAACAGC *AAAAAGAAAAATAAAAATTTTTTTT* TTAATTAA TCTT GGGCCC

L2bulge9.
5′CTCGAG GCGATCGC *AAACAAACAAA* GCTGTCACCG-GATGTGCTTTCCGGTCTGATGAGTCCGTTGTCCAATAC-CAGCATCGTCTTGATGCCCTTGGCAGTGGATGGGGAC-GGAGGACGAAACAGC *AAAAAGAAAAATAAAAATTTTT-TTT* TTAATTAA TCTT GGGCCC

L2bulge18tc.
5′CTCGAG GCGATCGC *AAACAAACAAA* GCTGTCACCG-GATGTGCTTTCCGGTCTGATGAGTCCGTTGTCCAAAAC-ATACCAGATTTCGATCTGGAGAGGTGAAGAATTCGAC-CACCTGGACGAGGACGGAGGACGAAACAGC*AAAAAGA-AAAATAAAAA* TTAATTAA TCTT GGGCCC

Inactive ribozyme.
5′CTCGAG GCGATCGC *AAACAAACAAA* GCTGTCACCG-GATGTGCTTTCCGGTACGTGAGGTCCGTGAGGACAGA-ACAGC *AAAAAGAAAAATAAAAATTTTTTTT* TTAATTAA TCTT GGGCCC

Controlling for toxicity and nonspecific effects of nucleofection and small-molecule ligand inputs on growth and gene expression. Gene expression can be sensitive to a myriad of external factors, and accurate characterization of phenotypic responses, such as cell growth and viability, requires appropriate controls to account for potential nonspecific effects of experimental procedures applied to the cells. In particular, the toxicity and other nonspecific effects of transfection and small-molecule ligand addition were of concern in the characterization of the ligand-responsive, ribozyme-based regulatory systems described here. Careful controls were included in the experiments reported in this study to ensure accurate accounting of any potential nonspecific effects.

Like most T-cell lines, CTLL-2 cells cannot be effectively transfected by lipid-based transfection reagents. Therefore, electroporation with Amaxa Nucleofector technology is the method of choice for transfecting CTLL-2 cells. The trauma of nucleofection results in high cell mortality and affects the health of surviving cells. To account for the toxicity of nucleofection, all experiments conducted in this study included as a positive control cells nucleofected with a similar DNA construct harboring an inactive, scrambled ribozyme that lacks an attached aptamer. This control construct has no ribozyme-based knockdown activity and no ligand-responsive cleavage activity, and it represents the maximum possible expression level from the regulatory system. Viability and fluorescence data from all other samples were reported relative to those of the positive control treated with the same concentration of small-molecule ligand. It has been verified by multiple nucleofection experiments that nucleofection toxicities from similar DNA constructs purified in the identical manner are similar.

The reproducible agreement between two characterization methods—viability (a phenotypic response) and fluorescence (a measure of reporter gene expression)—provided further confirmation of ligand-responsive gene regulatory activity (Fig. 2 and Fig. S1). To verify that growth cytokine withdrawal (and not nucleofection toxicity) is responsible for the decrease in viability levels observed for cells transfected with active ribozyme switch constructs, transfected samples were split into two identical aliquots, one of which was fed with 100 U/mL of exogenous IL-2, a concentration that is sufficient to sustain healthy expansion of CTLL-2 cells during routine culture maintenance. The IL-2-treated samples had significantly higher viability levels compared to identical samples not treated with exogenous IL-2 (Fig. S9*A*). Furthermore, the inverse correlation between viability and ribozyme switch copy number disappears in the presence of exogenous IL-2, suggesting that the reduced viability at high switch copy numbers is specifically caused by more efficient gene expression knockdown and the resultant cytokine withdrawal in the absence of exogenous IL-2. In contrast, the addition of exogenous IL-2 does not affect fluorescence levels (Fig. S9*B*). Taken together, these results indicate that the observed variations in viability levels are specific to the regulatory systems.

The toxicity and potential pleiotropic effects of the small-molecule ligands theophylline and tetracycline were also considered. In transient transfection experiments the fluorescence and viability values of all samples were normalized to that of the inactive ribozyme control treated with the same concentration of the small-molecule ligand (as described above) to account for non-aptamer-mediated effects of the ligand, as it is assumed that the nonspecific effects of the ligand will be similar for the sample and the control. Negative controls, such as cells transfected with vectors that encode either no growth cytokine or a growth cytokine gene coupled to a fully active, nonswitch hammerhead ribozyme control (sTRSV), were included in all transient transfection experiments. The relative viability and fluorescence levels from the negative control samples exhibited no response to ligand addition, indicating that the normalization method adequately accounts for the toxicity and pleiotropic effects of the small-molecule ligands (Fig. 2*B* and Fig. S1*A*).

By using the inactive ribozyme as the normalizing control for all switch constructs in all transient transfection studies, we report the regulatory output of the switches relative to the maximum possible expression range. Compared to the more commonly used method of internal normalization, where each switch construct is normalized to its own internal high value, our method has the effect of reducing the apparent dynamic range of each switch. However, the reporting of switch output to a consistent standard control allows for direct and accurate comparison of the various switches, which is important for system development and characterization. The internal normalization method is employed for in vitro gene expression assays on stably integrated cell lines (Figs. 3*B* and 5 and Fig. S5*A*), because the maximum expression level of each clone is dependent on the integration site, which varies from clone to clone.

In the characterization of cell lines stably expressing the ribozyme switch constructs, a clonal cell line expressing the positive control construct (inactive ribozyme) was included to identify any nonspecific effects of theophylline. As an example, an in vitro growth assay was performed on clonal cell lines in the presence or absence of 500 μM theophylline. The cell line expressing the inactive ribozyme exhibited a decreased growth rate in the presence of theophylline (Fig. S9*C*), indicating theophylline toxicity and verifying that the theophylline-induced increase in absolute growth rate observed from clones expressing the active ribozyme switches were not because of any nonspecific growth-stimulatory effects of theophylline (Fig. 3*A* and Fig. S4). As another example, positive and negative control cell lines were included in the animal studies and no significant theophylline-dependent differences were observed in the in vivo growth pattern of cells that either do not express growth cytokines or express the inactive ribozyme control (Fig. 4*A* and Fig. S6*C*). In contrast, the in vitro and in vivo growth rates of clonal cell lines expressing functional ribozyme switch systems show increases in absolute growth rate (not normalized to the inactive ribozyme control) in response to theophylline addition (Figs. 3*A* and 4*B* and Figs. S4 and S7). Taken together, these results indicate that the observed T-cell growth behaviors were specific to the ligand-responsive regulatory system.

1. Sambrook J, Russell DW (2001) *Molecular Cloning: A Laboratory Manual* (Cold Spring Harbor Press, Plainview, NY) 3rd Ed.

2. Livak KJ, Schmittgen TD (2001) Analysis of relative gene expression data using real-time quantitative PCR and the 2(-Delta Delta C(T)) method. *Methods* 25:402–408.

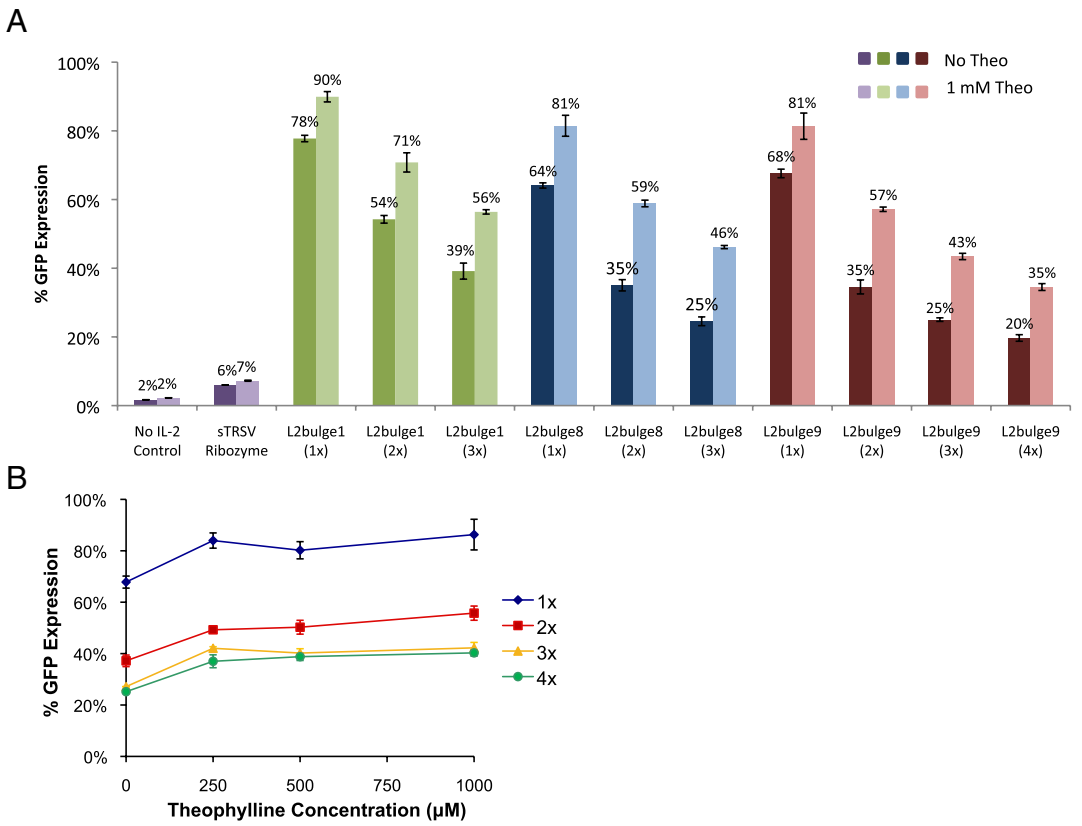

Fig. S1. Tunable, small-molecule-mediated regulation of gene expression in mammalian cells by ribozyme switches. (*A*) GFP expression levels are reported for constructs encoding theophylline-responsive switches (L2bulge1, 8, 9) in one (1×), two (2×), three (3×), and four (4×) copies through transient transfections in CTLL-2 cells grown in 0 and 1 mM theophylline. No IL-2 control, construct not encoding a proliferative cytokine; sTRSV Ribozyme, construct encoding a non-switch hammerhead ribozyme. (*B*) GFP expression levels are reported for multiple-copy L2bulge9 regulatory systems at various theophylline concentrations. Fluorescence values were normalized as described in Fig. 2. Values are mean ± SD from at least two replicate samples. Fluorescence and viability measurements yielded consistent results, thus validating the use of a fusion transgene as the regulatory target.

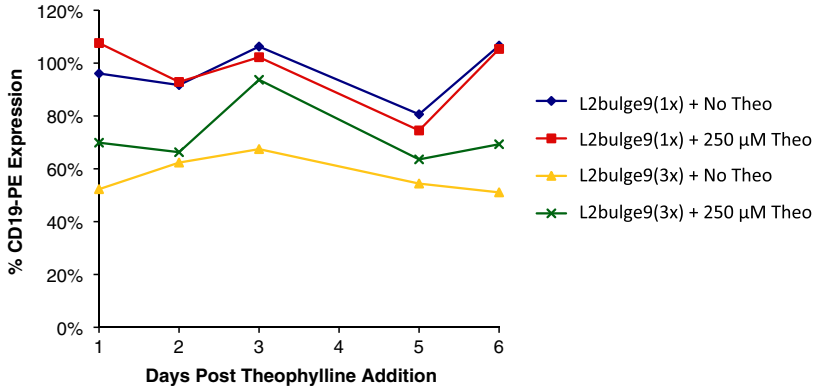

Fig. S2. Stable cell lines expressing multiple ribozyme switches exhibit lowered basal level and increased switch dynamic range. Stable integrants were selected by fluorescence-based cell sorting for CD19+ populations. Bulk-sorted cells were cultured either with or without 250 μM theophylline for 6 days and CD19 expression levels were monitored by staining with PE-conjugated CD19 antibodies. Although bulk cell lines stably expressing the single-copy ribozyme switch system did not exhibit significant increases in gene expression in response to 250 μM theophylline, individual clones that exhibited low basal expression levels and significant theophylline-responsive increases in expression were successfully isolated from this bulk population (see Fig. S4).

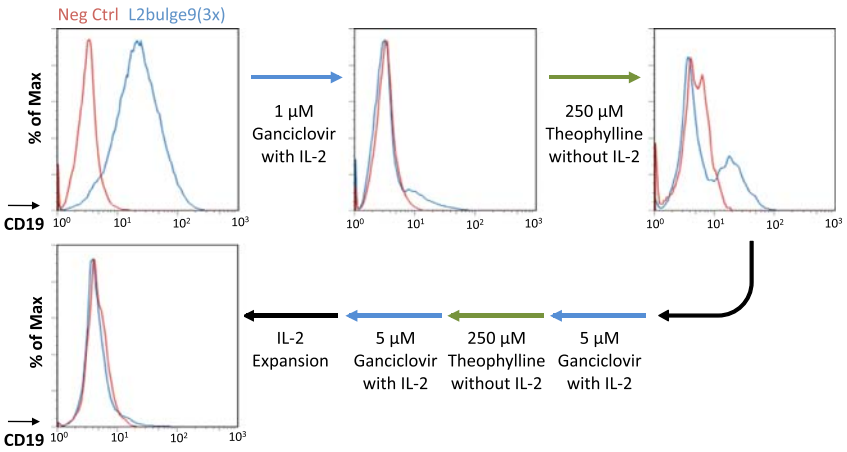

Fig. S3. The generation of T-cell lines stably expressing the ribozyme switch systems through alternate cycles of negative and positive selections. CTLL-2 cells stably expressing a luciferase reporter (CffLuc) were transfected with linearized plasmids encoding ribozyme switch systems on the basis of L2bulge9. Stable integrants were initially sorted for CD19 expression and subsequently subjected to alternate cycles of negative and positive growth selection with ganciclovir and theophylline, respectively. Gene expression levels were monitored by staining with PE-conjugated CD19 antibody; blue, bulk stable *cd19-tk-t2a-il15*-L2bulge9(3×) cell line; red, CffLuc cell line.

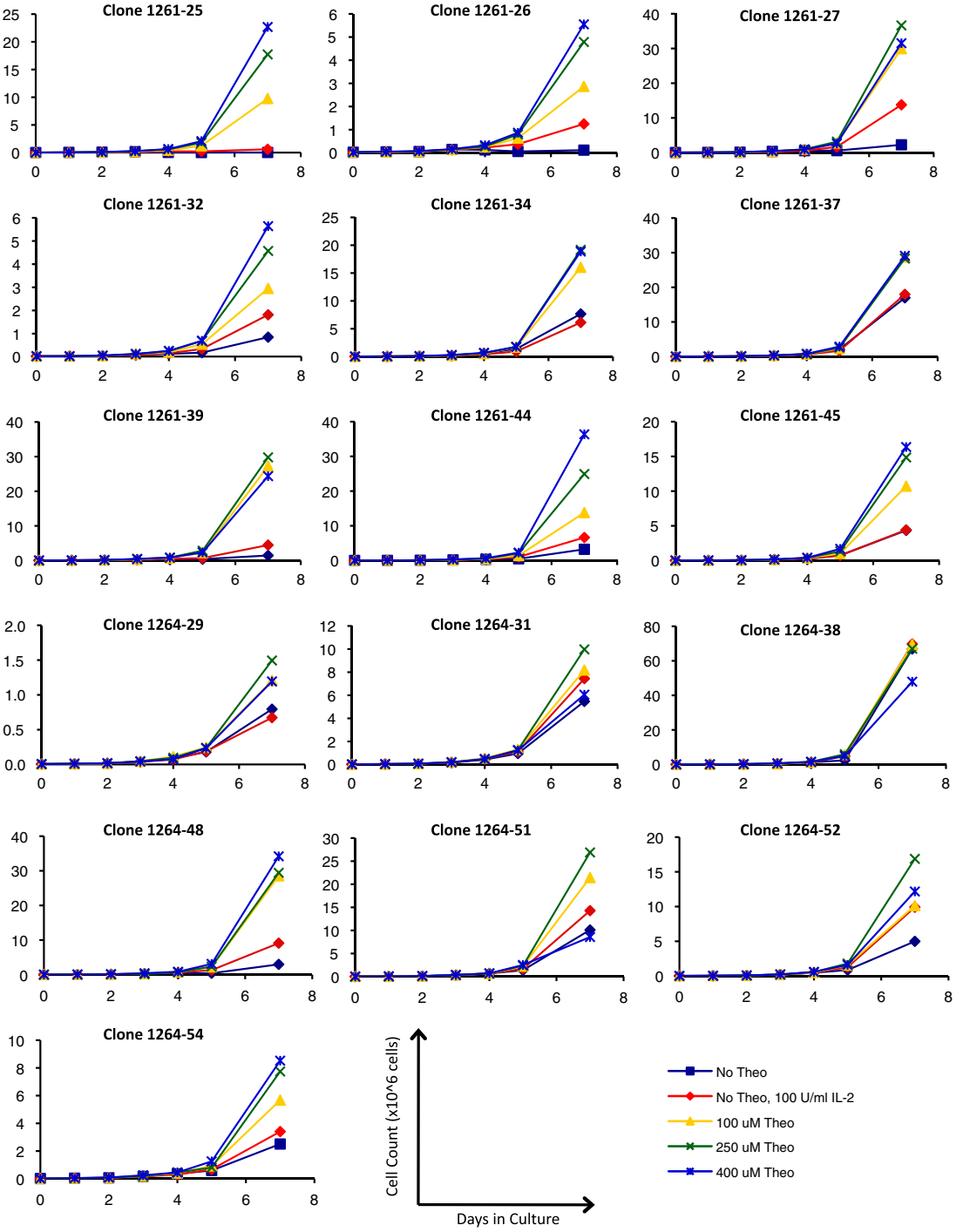

Fig. S4. Clonal CTLL-2 cell lines stably expressing engineered ribozyme switch systems exhibit effective theophylline-responsive growth regulation. The cell lines were cultured at various theophylline concentrations, and cell growth was monitored by counting viable cells. Clones indicated as 1261-xx stably expressed *cd19-tk-il15*-L2bulge9(1×). Clone 1264-xx stably expressed *cd19-tk-il15*-L2bulge9(3×). Growth behaviors differ from clone to clone, as would be expected from non-site-specific integration of the transgene into the host chromosomes. Theophylline-responsive increase in cell growth is evident in 15 of the 16 tested clones, and the growth elevation is statistically significant for the sample set ($P = 0.0150$, 0.0011, and 0.0013 for 100, 250, and 400 μM, respectively, by Whitney–Mann U test).

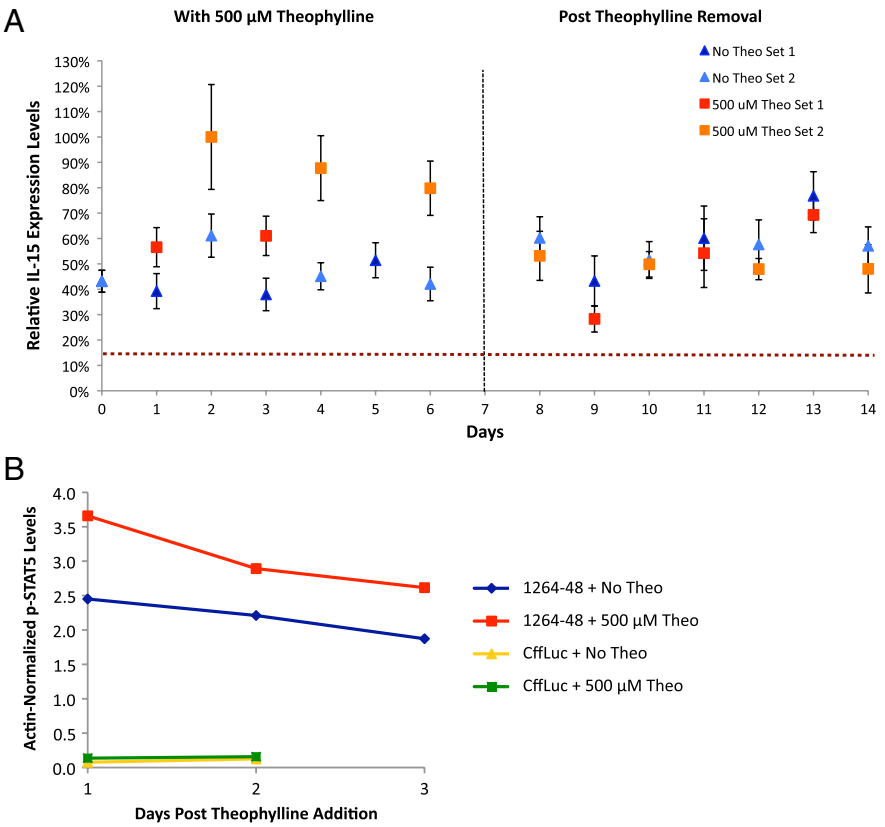

Fig. S5. Cells stably expressing the T-cell proliferation regulatory system exhibit theophylline-responsive increase in IL-15 transcription and signal transduction through the JAK-STAT pathway. (*A*) Relative IL-15 mRNA levels are elevated in the presence of theophylline and return to basal levels upon theophylline removal. qRT-PCR was performed on mRNA extracted from a CTLL-2 cell line stably expressing *cd19-tk-il15*-L2bulge9(3×) (clone 1264-48). IL-15 expression levels were normalized to expression levels of the housekeeping gene *hprt1*, and relative IL-15 expression levels were obtained by normalizing to the inactive ribozyme control. The highest expression level was set to 100%. Reported values are mean ± SD from three replicate samples. Samples shown in this figure were collected from the same cultures as described in Fig. 3*B*. The red dashed line indicates background signal from a cell line without a CD19 expression construct. (*B*) Western blot analysis was performed on protein extracts from the CffLuc and 1264-48 cell lines for phosphorylated STAT5 (p-STAT5), an intermediate in the IL-15 signaling cascade. The levels of p-STAT5 in each sample were normalized to that of β-actin. The 1264-48 cell line, which stably expresses *cd19-tk-il15*-L2bulge9(3×), showed increased p-STAT levels in response to theophylline, indicating an increase in IL-15 signaling. The CffLuc cell line, which lacks the ribozyme switch system, served as a negative control and verified that theophylline did not nonspecifically activate the JAK-STAT pathway. The CffLuc cell line could not survive beyond 2 days without exogenous IL-2, further demonstrating that the autocrine growth cytokine production is necessary for sustaining CTLL-2 survival and proliferation in the absence of exogenous cytokine supplies.

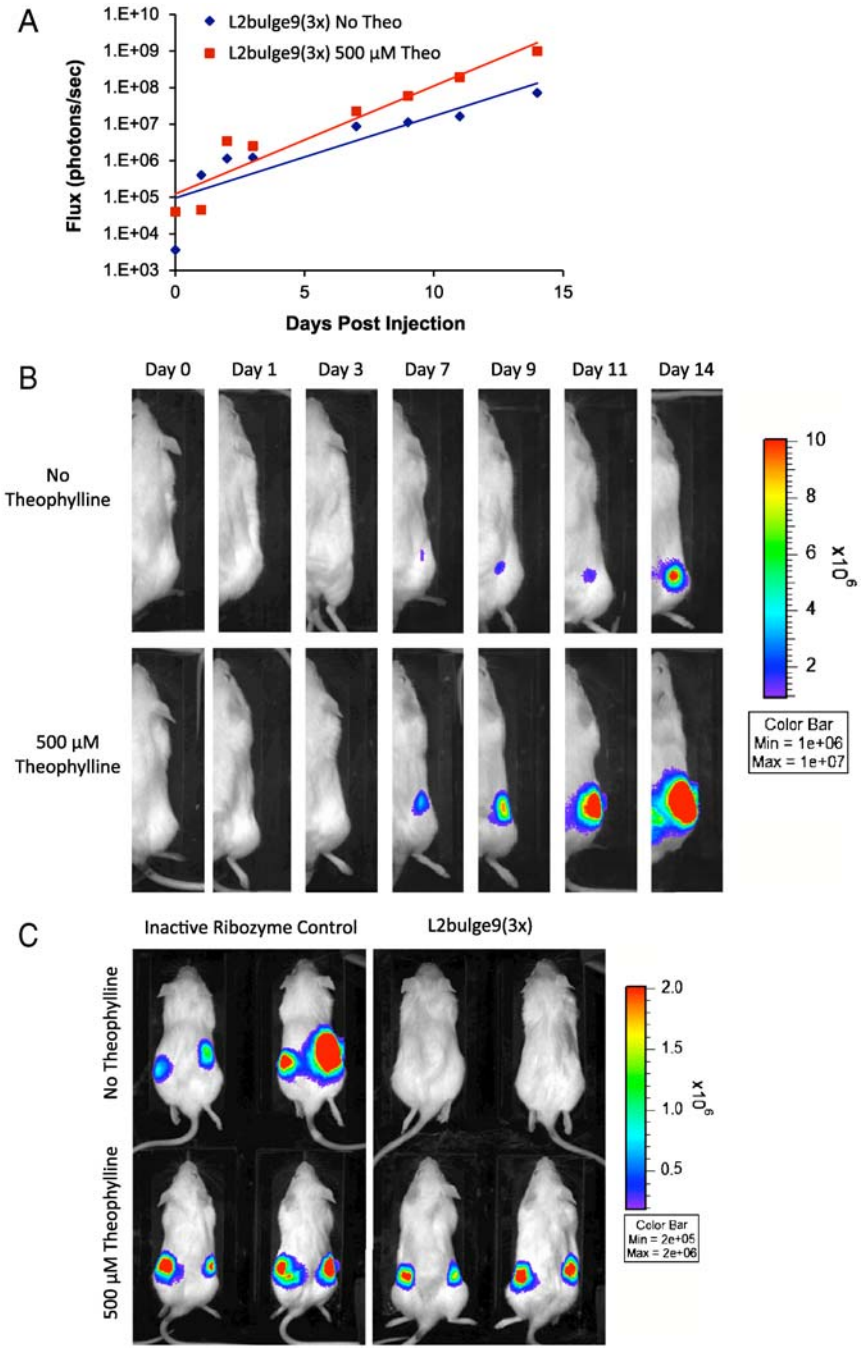

Fig. S6. Clonal cell line 1264-48 exhibits accelerated T-cell proliferation in response to small-molecule input. (*A*) Total luciferase signal flux measurements collected over a 14-day period were fitted to an exponential curve and used to calculate the in vivo growth rate of the injected cells. (*B*) Images of clone 1264-48 over time. The day of imaging postinjection of the stable cell line is indicated. (*C*) The ribozyme switch system demonstrates robust and reproducible small-molecule-mediated control over T-cell proliferation in vivo. Images are shown for day 4 postinjection of the positive control and clone 1264-48. Identical clones were injected into the two flanks of each mouse in the presence or absence of 500 µM theo.

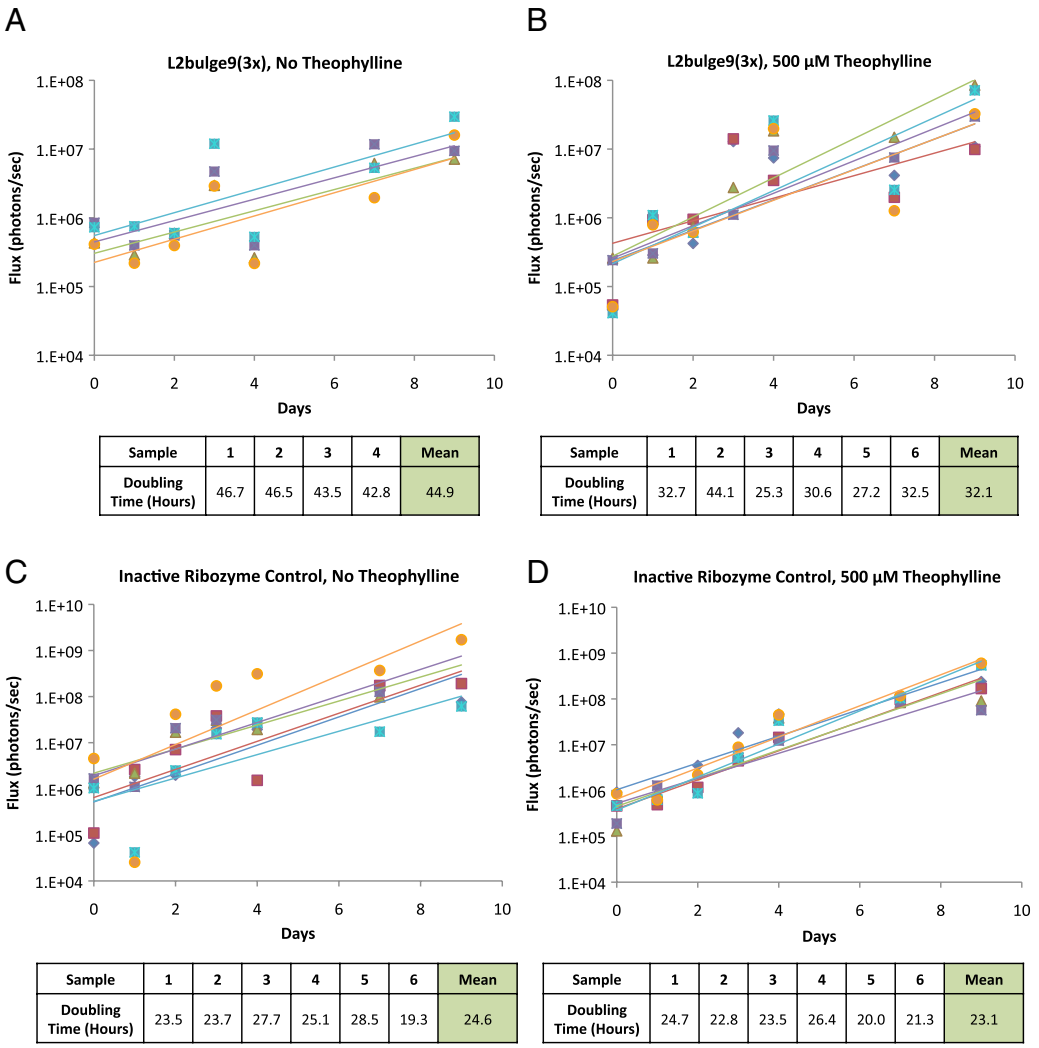

Sample	1	2	3	4	Mean
Doubling Time (Hours)	46.7	46.5	43.5	42.8	44.9

Sample	1	2	3	4	5	6	Mean
Doubling Time (Hours)	32.7	44.1	25.3	30.6	27.2	32.5	32.1

Sample	1	2	3	4	5	6	Mean
Doubling Time (Hours)	23.5	23.7	27.7	25.1	28.5	19.3	24.6

Sample	1	2	3	4	5	6	Mean
Doubling Time (Hours)	24.7	22.8	23.5	26.4	20.0	21.3	23.1

Fig. S7. A clonal cell line stably expressing a functional ribozyme-based regulatory system exhibits theophylline-responsive increases in the in vivo growth rate. Total luciferase signal flux measurements collected over a 9-day period from replicate mice were fitted to an exponential curve and used to calculate the in vivo growth rate of the injected cells. (*A* and *B*) Clone 1264-48 injected in the absence (*A*) or presence (*B*) of 500 μM theophylline. (*C* and *D*) Inactive ribozyme control cells injected in the absence (*C*) or presence (*D*) of 500 μM theophylline. Results indicate a 40% increase in the growth rate of clone 1264-48 in response to 500 μM theophylline and no statistically significant difference in the growth rate of the inactive ribozyme control in the presence and absence of theophylline.

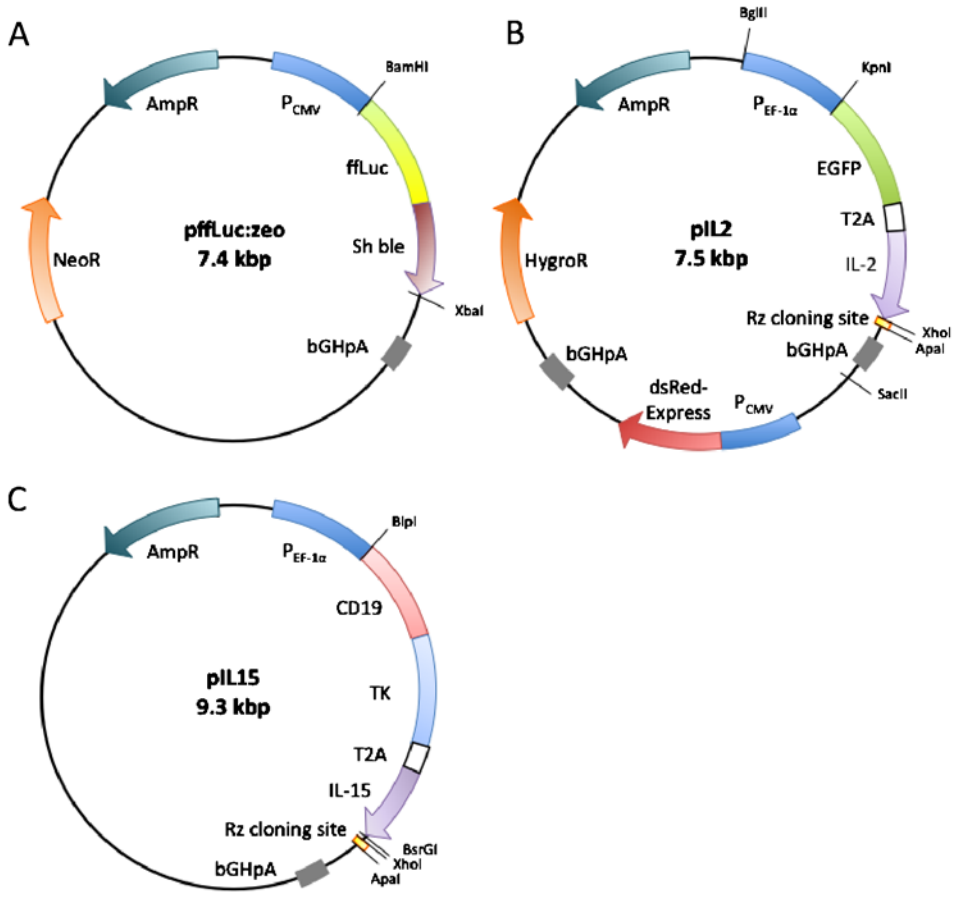

Fig. S8. Plasmid maps of T-cell proliferation constructs. (*A*) pffLuc:zeo was used in constructing T-cell lines stably expressing firefly luciferase for in vivo imaging; (*B* and *C*) pIL2 and pIL15 are the base T-cell proliferation expression constructs into which the ribozyme-based regulatory devices are inserted.

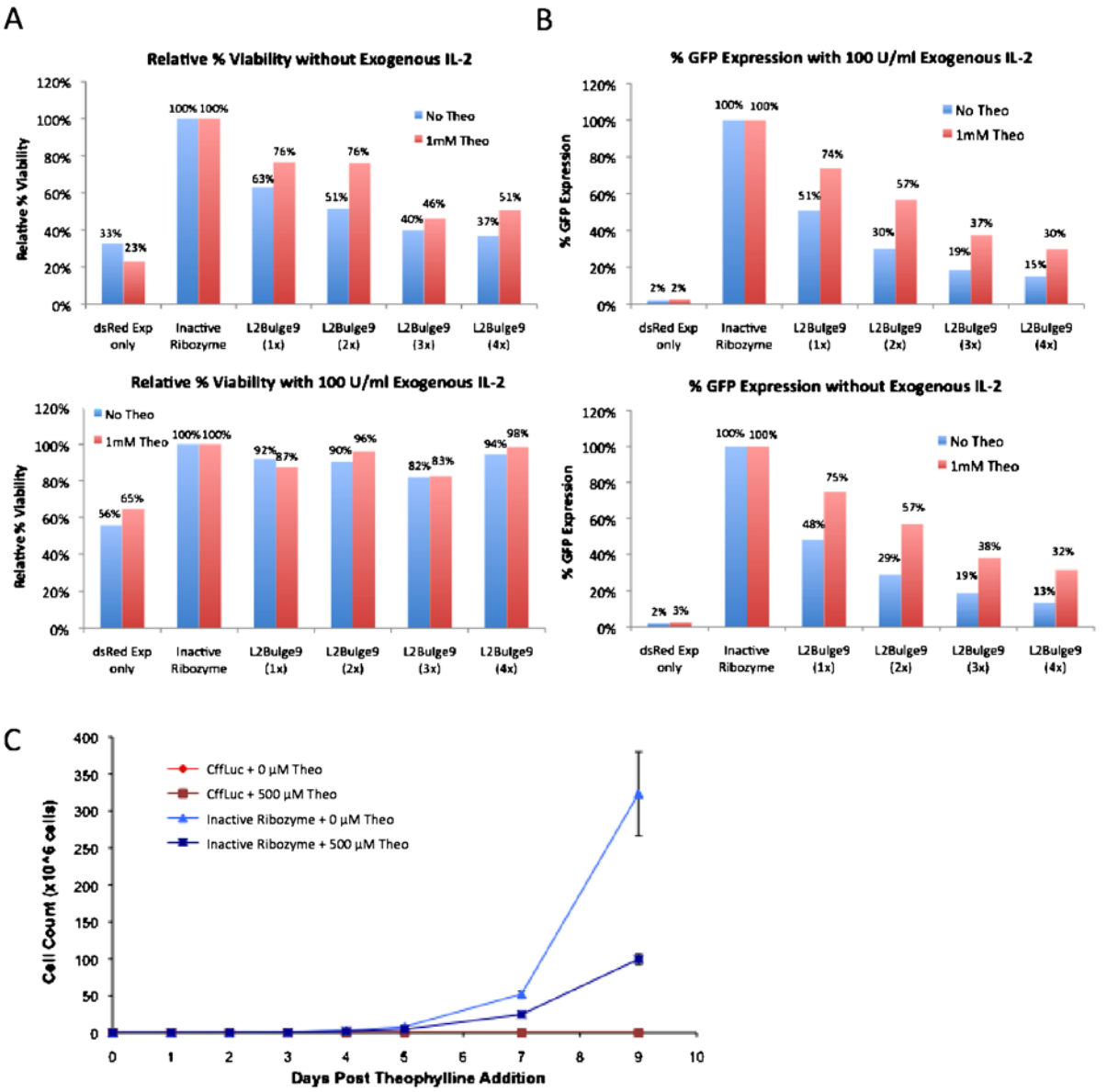

Fig. S9. Appropriate controls demonstrate observed ligand-responsive switch activities are because of specific effects of cytokine withdrawal. (*A*) Relative viability of CTLL-2 cells transiently transfected with ribozyme-based regulatory systems as measured by flow cytometry. The presence of exogenous IL-2 elevates viability in all samples and abolishes the inverse correlation between viability and ribozyme switch copy number observed in the absence of exogenous IL-2. These results suggests that the reduced viability at high switch copy numbers observed in the absence of exogenous IL-2 is specifically caused by more efficient knockdown of the cytokine transgene encoded by the regulatory system and the resultant cytokine withdrawal. (*B*) GFP expression in CTLL-2 cells transiently transfected with ribozyme-based regulatory systems. Fluorescence values were normalized as described in Fig. 2. The samples shown here correspond to those shown in *A*. In contrast to viability behaviors shown in *A*, switch activity as measured by fluorescence is unaffected by the presence of exogenous IL-2, indicating that the gene expression modulation is specific to the regulatory system. (*C*) Theophylline inhibits growth in CTLL-2 cells. CffLuc cells and a clonal cell line stably expressing the inactive ribozyme were cultured in the presence or absence of 500 µM theophylline without exogenous IL-2. Cell count was monitored for 9 days by flow cytometry. CffLuc cells failed to expand because of lack of growth cytokines. The inactive ribozyme control, which expresses high levels of cytokine independent of theophylline, showed reduced growth in the presence of theophylline, indicating theophylline toxicity.